Theor Chem Acc (2012) 131:1093
DOI 10.1007/s00214-012-1093-2

REGULAR ARTICLE

Exploration of conformations and quantum chemical investigation of L-tyrosine dimers, anions, cations and zwitterions: a DFT study

Uppula Purushotham · G. Narahari Sastry

Received: 25 April 2011 / Accepted: 5 July 2011 / Published online: 9 February 2012

Abstract Conformational analysis of tyrosine (**YN**) and its ionized counter parts cations (**YC**), anions (**YA**) and biologically relevant zwitterionic form (**YZ**) has been carried out. An exhaustive and systematic exploration of L-tyrosine dimer (**YD**) conformations resulted in about 59 distinct minima on the potential energy surface. The hydrogen bonds and a variety of non-covalent interactions such as OH–π, NH–π, CH–π, CH–O and π–π interactions stabilized the different forms of tyrosine and its dimers. Atoms in molecules analysis was performed to evaluate the nature and strength of the non-covalent interactions. Over all the NH–O, hydrogen bonds have showed higher stability than other non-covalent interactions in this study. The most stable dimers predominantly possess hydrogen bonding interactions, while the ones with aromatic side chain interactions are less stable. A delicate balance of non-covalent interactions governed the stability of different forms of tyrosine and its dimers.

Keywords Aromatic amino acids · DFT · AIM analysis · Zwitterion · Ionized counter parts · Non-covalent interactions

Dedicated to Professor Eluvathingal Jemmis and published as part of the special collection of articles celebrating his 60th birthday.

Electronic supplementary material The online version of this article (doi:10.1007/s00214-012-1093-2) contains supplementary material, which is available to authorized users.

U. Purushotham · G. Narahari Sastry (✉)
Molecular Modeling Group, Indian Institute of Chemical Technology, Tarnaka, Hyderabad 500 007, India
e-mail: gnsastry@gmail.com

1 Introduction

Twenty naturally occurring L-amino acids are building blocks of the proteins, and they are distinguished by their different side chain structures and chemical compositions. They contribute to the specificity of molecular recognition secondary structure and hydrophobic core formation in protein folding. Tyrosine (**YN**) is a non-essential, polar aromatic amino acid. The body converts phenylalanine in to **YN** by the metabolism of phenylalanine hydroxylase enzyme, which is extremely important as a precursor for catecholamines such as dopamine, norepinephrine and epinephrine neurotransmitters [1]. Tyrosine also helps in melanin (the pigment responsible for hair and skin color) production and in the function of organs, which are responsible for making and regulating hormones, including adrenal, thyroid and pituitary glands. Tyrosine deficiency results in partial or complete albinism, hypothyroidism and low blood pressure [2]. Understanding the structural preference and stability of tyrosine and its ionized counterparts anions, cations and zwitterions is of outstanding importance in its own right.

Around two decades ago, Levy's group reported the first gas-phase electronic spectra of phenylalanine and tyrosine in a supersonic jet-using laser induced fluorescence spectroscopy and proposed ten unique conformers and named conformers from A to J [3]. Toennies and coworkers proposed only four peaks in their He droplets experiment [4]. Li et al. [5] found only E, I and J, and given in the spacing E, H, I and J could be a repeat of A, B, C and D with an energy difference of 123 cm^{-1}. Levy et al. interpreted the above pattern as arising from OH group splitting [3]. The laser desorption resonant two photon ionization (LD-R2PI) spectrum of tyrosine agreed quite well with Levy's work by means of a hole-burning experiment [6]. Finally, Cohen

et al. [7] assigned the origins for A, C, D, D8, F and G to the conformers in which the ring and chain are gauche to each other and that for B, B8, E and E8 to anti conformers. The $NH_4^+$and NMe_4^+ions have shown NH–π and CH–π interactions with the aromatic motifs, herein the interaction energies of NH–π and CH–π complexes are higher than hydrogen bonding interactions; thus, the orientation of aromatic side chains in protein is effected in the presence of cations [8, 9]. The conformational analysis of a gaseous **YN** molecule has been carried out by Lin et al. using density functional theory (DFT) calculations, who found the involvement of hydrogen bonding between the carboxylic and amino groups and interaction between the amino group and π-electrons of the phenol ring [10–12]. Qualitative effect of non-bonded interactions and how the non-bonded interactions mutually influence each other are topic of great contemporary interest.

Experimental techniques such as mass and laser spectroscopy were of high utility to study the charged aromatic amino acids. Based on the infrared spectra and DFT calculations, Stearns et al. [13] reported four conformations of protonated tyrosine (**YC**) in their experiment, all of which are stabilized by hydrogen bonding between the charged NH_3^+ group and the aromatic ring and carbonyl oxygen. Boyarkin et al. [14] compared the temperature-dependent photo fragmentation spectra of protonated tryptophan ($TrpH^+$) and **YC**. In comparison with $TrpH^+$, the electronic excited state of **YC** was found to be substantially stable. Similar observations have been made in a pump–probe photo fragment study performed by Kang et al. [15], and they described the difference in the decay time scales of two protonated amino acids as the difference in the coupling strength between π–π^* and π-σ^* states. The high-level ab initio coupled-cluster calculations explained the longer excited state lifetime of tyrosine by the larger gap between the locally excited π–π^* and the dissociative π-σ^* states [16]. Many possible protonation sites exist for amino acids and this is a topic of interest to experimentalists and theoreticians [17]. High intrinsic hydrophilicity, charge-dipole, dipole–dipole interactions among water molecules and the lack of alternative fully exposed hydration sites are reported to be responsible for the high water affinity of carboxyl group than ammonium group [18].

While the studies on the negatively charged tyrosine or aromatic amino acids in general are scarce as the C-terminus has been assumed the site of deprotonation for all amino acids, recently deviations have been reported for the conjugated bases of cystine and tyrosine [19–21]. Calculations of de protonated cystine ($CysH^-$) and tyrosine (**YA**) showed that deprotonation occurs at the side chain rather than at C-terminus [22], and it was supported by the gas-phase acidities by H/D exchange experiments [23]. Gas-phase IR spectroscopy and DFT studies of amino acids (Asp, Cys, Phe, Ser, Trp and **YN**) suggest that all gas-phase amino acids adopt a carboxylate structure upon deprotonation [24].

The neutral-to-zwitterions transition of amino acids is a prime example of biological phenomena triggered by the presence of water. The existence of zwitterionic moieties of amino acids is very uncommon without presence of any intermolecular interactions, explicitly from water molecule, or any other polar ligands such as fluorine, alkali and alkaline earth metal cations [25]. Zwitterionic forms may be stabilized by the addition of a proton, an electron, a metal cation, or a metal dication or by microsolvation [26]. There is no consensus among the theoretical studies of micro-hydrated amino acids concerning the amount of water required to stabilize the zwitterionic form it ranges from two to four H_2O molecules [27]. Recently in literature, the formation of an autozwitterion by intramolecular proton transfer between nearby residues in a neutral and isolated peptide has been reported [28]. Solvation seems to play a very significant role in altering the strength of non-bonded interactions substantially [27].

Understanding the interactions between amino acid side chains is of outstanding importance, as they play an important role, in protein folding and their stability. The extensive studies on the model systems such as benzene, phenol and toluene were carried out in last few decades to characterize the aromatic–aromatic interactions in the proteins [29]. Extensive ab initio studies show how the benzene dimers could adopt hypothetically similar geometrical rearrangements to those shown by aromatic side chains [30]. These studies indicate that T-shaped and parallel displaced structures are almost isoenergetic using high-level quantum chemical methods, whereas the parallel stacked conformation is higher in energy [31–33]. High-level ab initio calculations reveal the presence of a minimum energy structure for the phenol dimer in which the arrangement of molecules is perpendicular, but with one molecule donating an OH–O bond rather than an OH–π bond [34]. Sagarik and Asawakun [35] also predicted this structure using a potential-based test particle model [36], and it is in good agreement with experimental results [37]. As in toluene, stacked dimers of phenol are found to be more favorable than those of benzene [38]. Molecular dynamics simulations on tyrosine have found that the structure is largely perpendicular but that molecules stack over the OH group [39]. Experimental work has been performed to determine the distribution of tyrosine residues in proteins there studies revealed that while stacked residues were preferred at short separations, as the inter-residue distances increased a T-shaped arrangement became more favorable [40]. The ab initio dimerization energy landscapes of aromatic amino acids and proline side chains in proteins are fairly well reproduced by

empirical force fields and that the interaction between cyclic side chains contribute to the geometric distributions observed in protein structures [41]. Non-covalent interactions, such as cation–π, stacking and hydrogen bonding, are key to supramolecular aggregation, and computational studies provide valuable insights in this direction [42–47]. The cation–π interactions have emerged recently as an important member of the non-covalent forces involved in the structural and functional properties of proteins [48–55].

To our knowledge, a systematic conformational analysis of tyrosine dimers and monomers has not yet been reported. There are many questions to be answered such as (a) What are the conformational preferences and stabilizing factors of the tyrosine and its ionized counter parts? (b) What is the role of non-covalent interactions in the stability of this biologically important amino acid? (c) Which factors are influencing dimeric formation of tyrosine? (d) How are the energetics of tyrosine influenced by various method and basis sets applied? This study seems to address the above questions by a systematic analysis of L-tyrosine dimers, neutral monomers, cations, anions and zwitterions at M05-2X and B3LYP levels of theory with using 6-31G(d) and cc-pVTZ basis sets. It is of fundamental interest to study the dimeric forms of amino acids in general and aromatic amino acids in particular to assess the possible conformations and their stability [56]. Dispersion corrections have also been carried out at B3LYP level of theory using cc-pVTZ basis set. Atoms in molecules (AIM) analysis carried out to analyze the capability and strength of the non-bonded interactions.

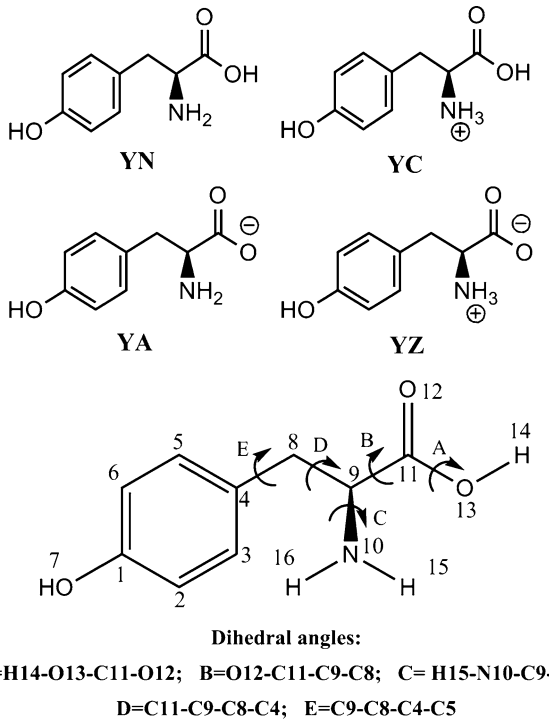

Scheme 1 The systems considered in this study and representation of dihedral angles, which are considered for the generation of tyrosine conformations

2 Computational details

The conformational space of L-tyrosine monomer (**YN**) has been explored through a systematic variation of five dihedral angles (Scheme 1); the fifth dihedral angle E was kept constant as 90°. A series of trial structures were generated by allowing possible combinations of internal single-bond rotamers. Initially, the optimization of 235 trial conformations at B3LYP/6-31G(d) level resulted in 38 stationary points and frequency calculations at B3LYP/6-31G(d) level characterized the unique 38 conformers as minima on the potential energy surface (PES). These 38 unique conformers of neutral tyrosine were further used to generate the cations (**YC**), anions (**YA**) and zwitterions (**YZ**) of tyrosine by adding and removing hydrogens. Initial optimizations of **YA**, **YC** and **YZ** trial conformers at B3LYP/6-31G(d) level of theory eventually resulted 12, 14 and 9 unique conformations on PES of **YA**, **YC** and **YZ,** respectively. Further frequency calculations at same level of theory characterized these conformations as minima on the PES. We have validated the conformational space of all the monomers by using highly sophisticated methods Conf. Gen module of Schrodinger and Discovery Studio. The initial optimizations of trial conformers generated by these modules have been carried out at B3LYP/6-31G(d) level of theory. The resulting conformers are similar and collapsed to the existing conformers. All the monomers subjected to further optimization at M05-2X/6-31G(d) and M05-2X/cc-pVTZ level of theories. In order to see the effect of augmented basis sets on anions and zwitterions, we have performed single point calculations at M05-2X/aug-cc-pVTZ//M05-2X/6-31G(d) level of theory. The zwitterionic conformations of **YZ** could not be obtained in the gas phase; however, they could be located only in the solvent phase, and we have been used polarizable continuum model (PCM) [57] calculations to locate the zwitterions. All possible conformations of D-tyrosine have also been explored at B3LYP/6-31G(d) level of theory in the current study (optimized geometries provided in the supporting information).

The conformational space of dimers has been explored by considering the relative orientation of two aromatic moieties such as parallel displaced, T-shape and stacked orientations and the possible hydrogen bonding interactions between COOH and NH_2 groups and also other non-covalent interactions between aromatic rings and COOH,

NH_2 groups such as OH–π, NH–π and π–π interactions. We have validated the conformational space of phenylalanine dimers by generating the conformations using Conf. Gen module of Schrodinger and Discovery Studio modules. Initially, the geometry optimization for trial conformations of **YD** was performed at M05-2X/6-31G(d) level of theory, which resulted in the identification of 59 unique conformers that were further characterized as minima on the potential energy surface (PES) of **YD**. Further single point calculations were performed at M05-2X/cc-pVTZ, MP2/6-31G(d) and Grimme empirical model in combination with the B3LYP hybrid method B3LYP-D/cc-pVTZ level of theory to added issue of dispersion corrections on M05-2X/6-31G(d) geometries [58, 59]. The computed interaction energies have been corrected for basis set super position error (BSSE) by using Boys–Bernardi counterpoise correction [60]. The interaction energy of **YD** was evaluated as the difference between the energy of complex (E_D) and monomer (E_M). We have also calculated the interaction energy as the difference between complex and individual monomers of respective complexes. The E_{M1} and E_{M2} are the energies of individual monomers of the respected complex **YD** at M05-2X/6-31G(d) level of theory in the gas phase, herein we have considered the fixed geometries of monomers in the respective dimers, and the single point calculations have been performed on those geometries at M05-2X/6-31G(d) level of theory. Those single point energies are considered as E_{M1} and E_{M2} energies. The following equations IE1 and IE2 are used to calculate interaction energy. The reorganizational energy (RE) of **YD** was calculated as the difference between the interaction energies IE1 and IE2 as given in the following equation.

$$\mathrm{IE1} = E_D - 2 \times (E_M) \quad (1)$$

$$\mathrm{IE2} = E_D - (E_{M1} + E_{M2}) \quad (2)$$

$$\mathrm{RE} = \mathrm{IE1} - \mathrm{IE2} \quad (3)$$

The Bader's AIM analysis was carried out to analyze the non-covalent interactions in monomers and dimers. The nature of bonding can be characterized by examining the value of electron density (ρ) and sign of Laplacian of electron density ($\nabla^2\rho$) at the bond critical point (BCP) and ring critical point (RCP). The bond critical points are characterized by a rank of 3 and signature of -1. This means that the electron density at this point has a minimal value in two orthogonal directions. The RCP (3, +1) is the eigenvectors associated with the two positive eigenvalues of the Hessian matrix of p at this critical point generated an infinite set of gradient paths. AIM analysis was carried out using the AIM 2000 program [61]. In this study, all calculations were performed using Gaussian 03 version E suite of program [62].

3 Results and discussion

3.1 Neutral tyrosine (YN)

The initial geometry optimization of 235 trial conformers was subjected at B3LYP/6-31G(d) level followed by frequency calculations. Many of the putative conformers collapsed to already existing ones resulting in the identification of 38 distinct stationary points characterized as minima on the potential energy surface of neutral monomer (Fig. 1). Figure 2 shows the variation of relative energies of **YN** at various levels of theory. **Y1** and **Y38** are identified as the most and least stable conformations in this study. At M05-2X level, the relative energy predicted using the cc-pVTZ basis set is slightly lower (0.26–1.16 kcal/mol) when compared with those predicted using the 6-31G(d), though in both the cases, the trends in the relative energy ordering remain virtually similar. The above analysis reveals that the energetics of the neutral conformations is not sensitive to the quality of the basis set employed. The relative energy of various conformations of neutral tyrosine at different levels of theory is given in the supporting information (SI) Table S7. Figure 1 shows the principal geometrical parameters and electron density (ρ) values at bond critical points (BCP) characterized by AIM analysis of various conformations of tyrosine at M05-2X/cc-pVTZ level of theory. Expectedly, the intra molecular interactions such as hydrogen bonding (HB), NH–π and OH–π interactions play an important role in stabilization of **YN**. The presence of two hydrogen bond donors (COOH and NH_2) and three hydrogen bond acceptors (C=O, COOH and NH_2) in **YN** allows for a wide range of hydrogen bonding combinations and consequently a large number of stable conformers. Herein, OH–N (**Y1**, **Y2**, **Y3** and **Y4**), NH–O (**Y5** and **Y6**), NH–OH (**Y7** and **Y8**) and OH–O (**Y8**, **Y9**, **Y14** and **Y15**) type of hydrogen bonds stabilize the **YN** conformations. The most stable conformations **Y1** and **Y2** are stabilized by the presence of a strong hydrogen bond between the hydroxyl group of COOH (proton donor) and the amino group (proton acceptor). In addition to these interactions, these conformations also exhibit NH–π and a weak non-bonded interaction between the aromatic C–H and COOH group CH–O interactions. The next most stable conformations **Y3** and **Y4** exhibit hydrogen bonding between COOH, NH_2 groups and NH–π interactions, and the weak non-bonded interaction CH–O is lacking in these conformations. The conformers **Y5**–**Y8** exhibit bifurcated hydrogen bonds between NH_2 and COOH group, these conformers differed only in the type of hydrogen bonding (NH–O) with most stable conformers (OH–N) this indicates that nitrogen is a good hydrogen bond acceptor than oxygen. Herein, **Y5**–**Y6** and **Y7**–**Y8** conformers are differed only

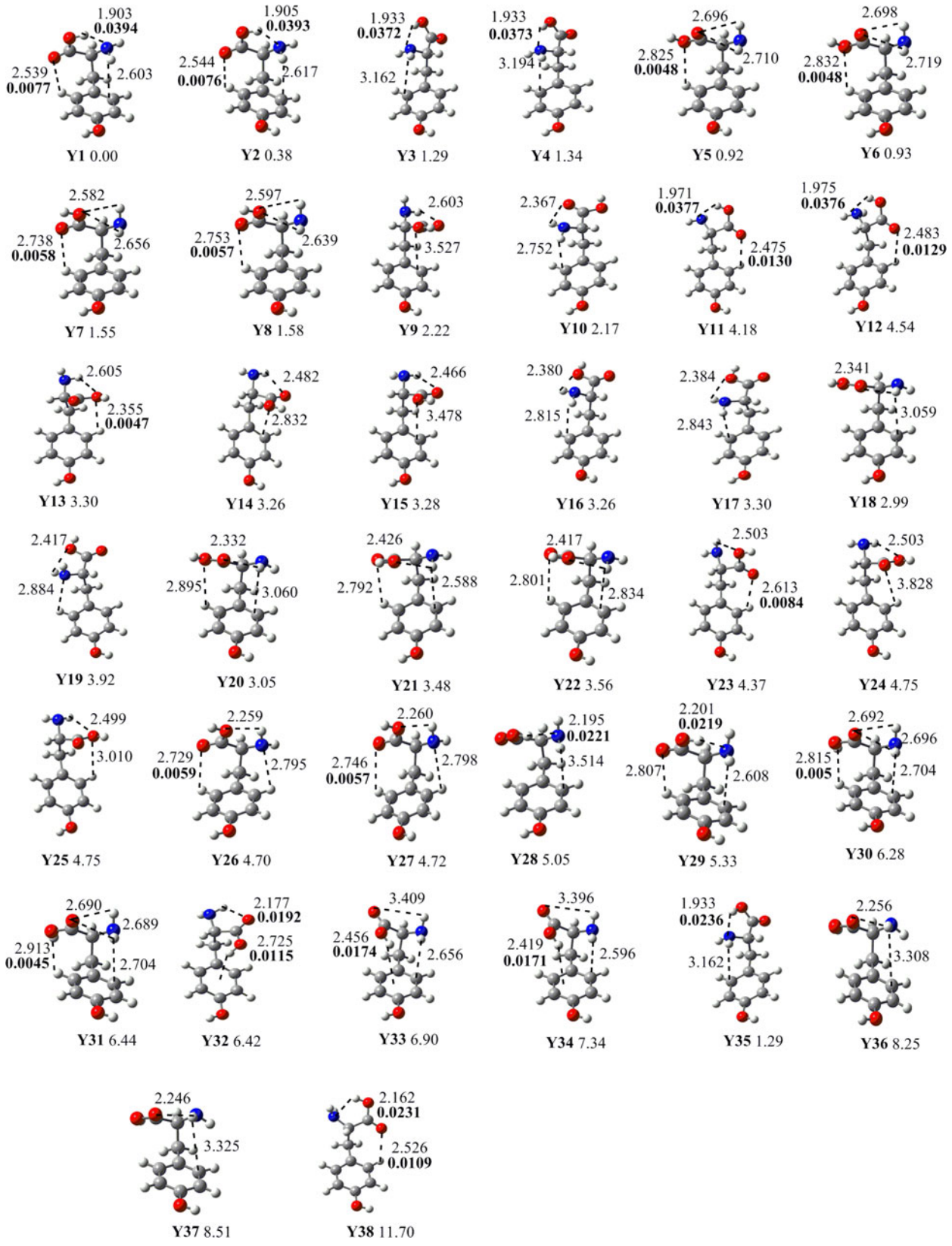

Fig. 1 The principal geometrical parameters (in Å), electron density rho (ρ in a.u. bold) at bond critical points in the case of specified geometries characterized by AIM analysis and relative energy (in kcal/mol) of various conformations of **YN** at M05-2X/cc-pVTZ level of theory

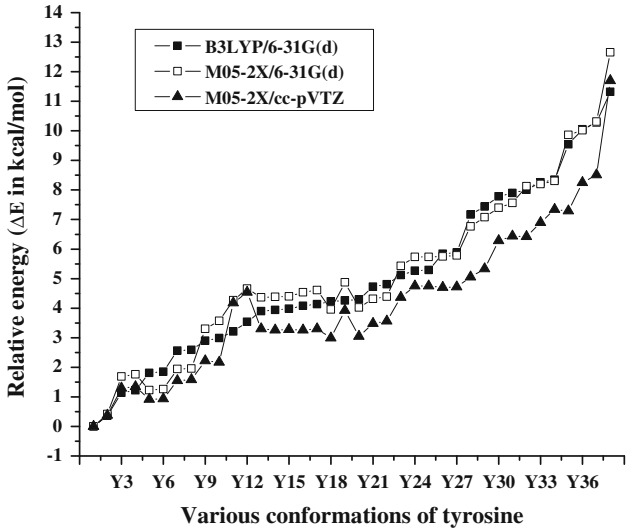

Fig. 2 The relative energy (ΔE in kcal/mol) of various conformations of **YN** with respect to **Y1** at different levels of theory

from the orientation of carboxylic group interaction with amino group; this shows the relative weakness of the interaction between the amino group and hydroxyl rather than the carbonyl oxygen atom. In the cut off range of 2.80 Å to near-atom interactions, all conformations except **Y33** and **Y34** showed intra molecular hydrogen bonds, between COOH and NH_2 groups (Fig. 1). Due to the OH group on aromatic ring, tyrosine conformations appeared in pairs. However, the OH group is not responsible for any intramolecular interactions; it splits the conformations in to pairs due to its two possible orientations. Herein, out of 38 conformers, 26 conformations are paired up to 13 pairs; all these conformations differ only in the orientation of OH group with virtually similar energy. Baders AIM analysis has been performed to see the strength and stability of various non-covalent interactions in **YN**. This analysis gave BCP and ring critical points (RCP) at OH–N, CH–O and CH–OH hydrogen bonds. However, no BCP and RCP were found for the H-bonds of NH–O, NH–OH or OH–O, this indicates that the type of interactions is not true HBs according to the AIM theory. The criteria for ρ and $\nabla^2\rho$ proposed at BCPs for the conventional H-bonds. Both parameters for closed-shell interactions as H-bond fall within the following ranges: 0.002–0.035 a.u. for the electron density and 0.024–0.139 a.u. for its Laplacian [63]. For most of the hydrogen bonds appeared in this study, ρ and $\nabla^2\rho$ values fall in the relative proposed ranges (0.0045 to 0.0394 a.u.). The rho values at BCPs have been reported in Fig. 1 shows that the higher values at OH–N hydrogen bond BCPs compare to other BCPs; this indicates that OH–N HBs are stronger than other non-covalent interactions appeared in this study. The above analysis reveals that a critical balance of non-covalent interactions modulates the stability of tyrosine conformations.

3.2 Tyrosine cation (**YC**)

The cations for tyrosine were generated by protonating the amino group in the neutral conformer. Thus, thirty-eight cationic conformations were initially considered and subjected to geometry optimization in the gas phase at B3LYP/6-31G(d) level. Only fourteen distinct conformers, frequency calculations at B3LYP/6-31G(d) level of theory characterized all conformers as minima, were obtained as many of the reputed conformers converged to the same local minima. The presence of non-bonded interactions in the conformers was analyzed by performing AIM analysis. Figure 3 depicts the principal geometrical parameters, electron density (ρ) at bond critical points characterized by AIM analysis and relative energy of various conformations of **YC** at M05-2X/cc-pVTZ level of theory. The conformers **YC1** and **YC2** are isoenergetic, and most of the conformations have been found to be 4–20 kcal/mol higher in energy compared to most stable conformer**.** At M05-2X level of theory, the relative energy predicted using the cc-pVTZ basis set is slightly lower, when compared with those predicted using the 6-31G(d) basis set; however, in both the cases, the trends in the relative energy ordering remain virtually similar (Table S8 in SI). The critical observation of **YC** conformers shows that the intramolecular interactions such as hydrogen bonding, NH_3^+–π and CH–O interactions are stabilizing the tyrosine cations. Herein, NH–O and NH–OH hydrogen bonds were appeared. There is no conformer, which has OH–N/O type of hydrogen bonds. The most stable conformers, **YC1** have strong NH–O hydrogen bond, NH_3^+–π interactions, YC2 have additionally CH–OH interaction, and these conformations are differed in the orientation of COOH and NH_2 groups. The participation of the carbonyl or hydroxyl oxygen as proton acceptor in hydrogen bonding also determines the stability. The conformers **YC1** and **YC2**, where the carbonyl oxygen acts as the proton acceptor, are more stable than those **YC3** and **YC4** where hydroxyl oxygen acts as the proton acceptor. The appropriate orientation of the COOH group is also another factor; the conformers **YC1**–**YC6** have cis COOH group and have more stability, than the conformers **YC8**–**YC13** that have trans COOH group. A cursory look at all conformers of **YC** indicates that like **YN**, due to the orientation of OH group on aromatic ring, **YC** conformers also resembled in pairs. In this study, **YC3**–**YC5**, **YC4**–**YC6**, **YC10**–**YC12**, **YC11**–**YC13** and **YC14**–**YC15** conformers were paired up. These conformers are differing only in the orientation of

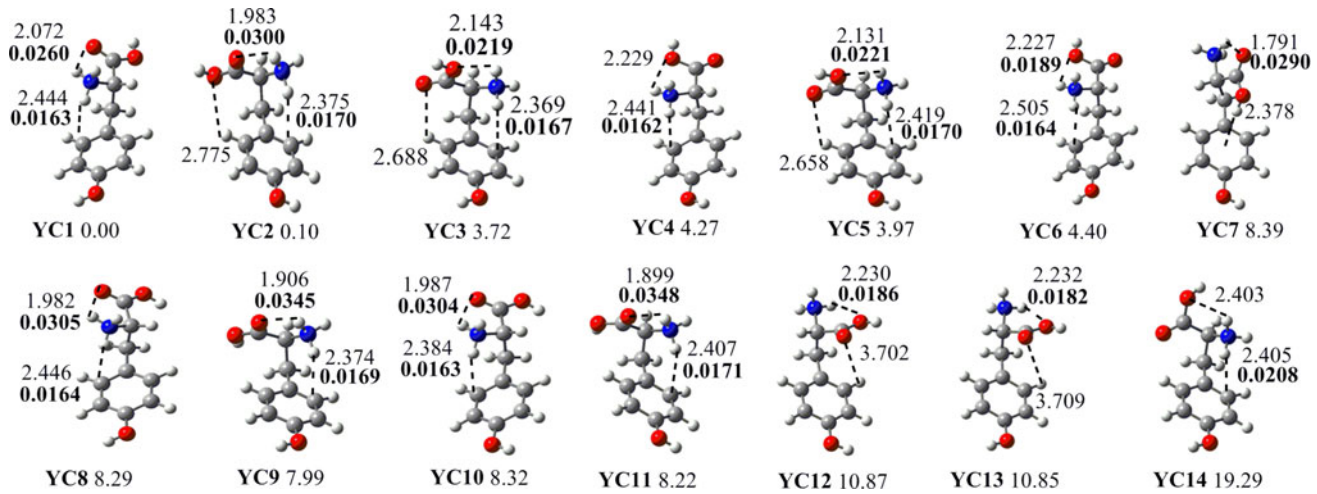

Fig. 3 The principal geometrical parameters (in Å), electron density rho (ρ in a.u. bold) at bond critical points characterized by AIM analysis and relative energy (in kcal/mol) of various conformations of **YC** at M05-2X/cc-pVTZ level of theory

aromatic OH group. Compare to **YN**, the **YC** conformers are clustered in the more energy difference. Herein, strong NH_3^+–π interactions are present that were absent in the case of **YN**. **YC1** have strong NH–O hydrogen bond, NH_3^+–π interactions. To analyze the non-covalent interactions in **YC**, we have been performed AIM analysis at B3LYP/6-31G(d) level of theory. The AIM analysis showed BCPs and RCPs at hydrogen bonds, NH_3^+–π and CH–O interactions. The (ρ) values are reported in Fig. 3 at particular BCPs. For most of the hydrogen bonds appeared in this study, the ρ values clustered in the range of (0.016–0.041 a.u.). The above analysis reveals that a susceptible balance of the non-covalent interactions administers the stability of tyrosine cations.

3.3 Tyrosine anion (**YA**)

The anions (**YA**) were generated by deprotonating the carboxyl group in the neutral conformers. Initially, the search for anionic conformers started with 38 putative structures that were subjected to geometry optimization and frequency calculation at the B3LYP/6-31G(d) level. This led to the identification of twelve unique conformers; the relative energies and principal geometrical parameters are presented in Fig. 4. The twelve stationary points obtained were characterized as minima on the potential energy surface. Herein, all the anionic conformations were clustered in below ~5.00 kcal/mol. The B3LYP/6-31G(d) predicts eight out of 12 conformers are in the

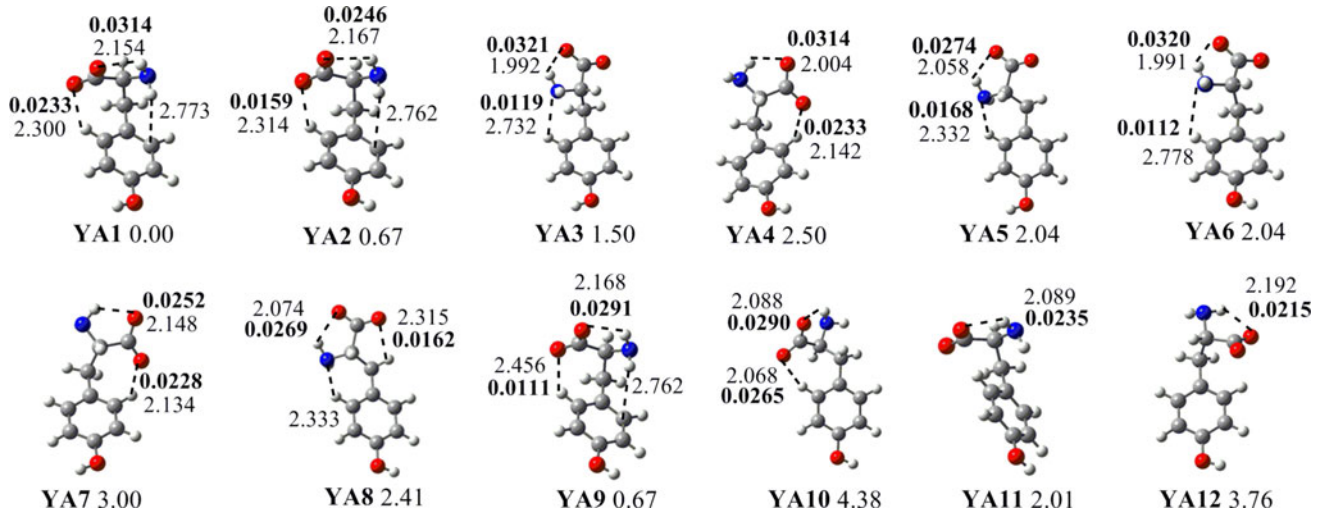

Fig. 4 The principal geometrical parameters (in Å), electron density rho (ρ in a.u. bold) at bond critical points characterized by AIM analysis and relative energy (in kcal/mol) of various conformations of **YA** at M05-2X/cc-pVTZ level of theory

range of 2.00 kcal/mol energy difference. Unlike cations, anions have clustered in less energy gap. A cursory look at all anions indicates that NH–O hydrogen bonds, NH–π and CH–O interactions are stabilizing tyrosine anions. Herein, we can observe one interaction between aromatic CH and nitrogen atom CH–N which is lacking in neutral and cationic conformations of tyrosine. The most stable conformers **YA1** and **YA2** are isoenergetic, and **YA1** and **YA12** are appeared as most and least stable conformations at all the levels of theories considered in this study. The most stable conformers stabilized by NH–O hydrogen bond, NH–π and CH–O interactions, remaining lower energy conformers are lacking some of the above interactions. A factor that is contributed to the stability is the conformers that have CH–O interactions (**YA1** and **YA2**) are more stable than the conformers (**YA4**, **YA7** and **YA9**) that have CH–N interactions. Anionic conformers also exhibited geometrical pairs as neutral and cationic conformers. All conformers paired up to six pairs, namely **YA1**–**YA2**, **YA3**–**YA6**, **YA4**–**YA7**, **YA5**–**YA8**, **YA9**–**YA11** and **YA10**–**YA12**. These conformers differ only in the orientation of the aromatic OH group. AIM analysis has been carried out to characterize the non-covalent interactions NH–O hydrogen bonds, NH–π and CH–O interactions. Figure 4 depicts the ρ values at bond critical points of anionic conformers. For most of the conformers, ρ values are clustered in the range of 0.0321–0.0159.

3.4 Tyrosine zwitterions (**YZ**)

Zwitterion constitutes the most important form in which amino acids exist in the nature. Amino acid exists in the neutral, non-zwitterionic form in the gas phase, while in the solvent phase, they generally exist as zwitterions. However, reports do indicate the presence of zwitterions of basic amino acids like arginine and histidine even in the gas phase [26, 64–66]. Hence, the search for the zwitterionic form of tyrosine was carried out both in the gas and solvent phase at B3LYP/6-31G(d) level of theory. All our attempts to locate the zwitterions of tyrosine in the gas phase were futile and resulted in the generation of **YN** due to the migration of proton from the ammonium ion to the carboxylate anion. In solvent phase, however, nine conformers of **YZ** could be located which were all characterized as minima on the potential energy surface. Relative energies and principal geometrical parameters of various conformations of **YZ** have been reported in Fig. 5. The conformers **YZ1**–**YZ4** were isoenergetic and put down to below 1 kcal/mol. Unlike other monomers, zwitterions are clustered in less energy gap; this shows the flat nature of zwitterionic conformations on PES. A cursory look at Fig. 5 indicates **YZ** conformers stabilizing by intramolecular hydrogen bonding between COOH, NH_3^+ groups, NH_3^+–π and CH–O interactions. The most stable conformer **YZ1** is stabilized by NH–O hydrogen bonding,

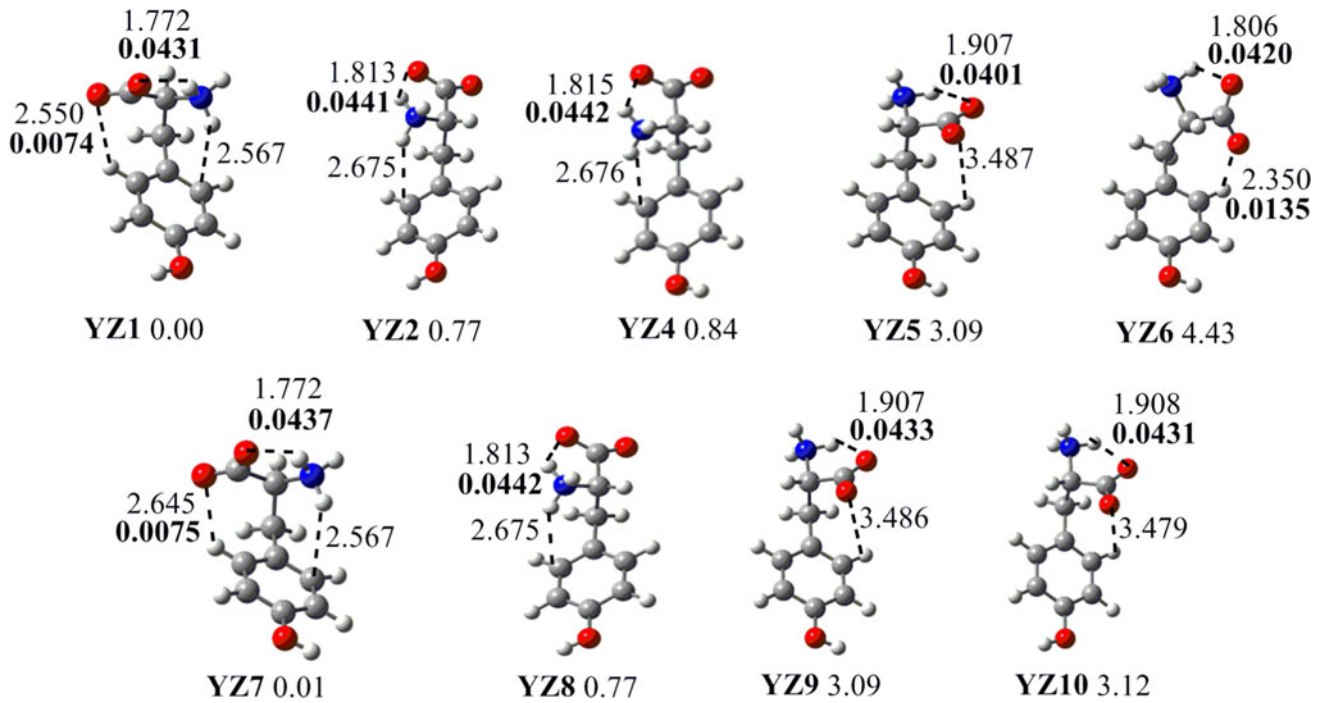

Fig. 5 The principal geometrical parameters (in Å), electron density rho (ρ in a.u. bold) at bond critical points and relative energy (in kcal/mol) of various conformations of **YZ** (in solvent phase) at M05-2X/cc-pVTZ level of theory

NH_3^+–π and CH–O interactions. The conformers **YZ2** and **YZ4** have only NH–O hydrogen bonding and NH_3^+–π interactions, and these indicate that weaker interaction CH–O is also responsible for the stabilization of **YZ** conformers. Another factor, which is responsible for stability, is NH_3^+–π interaction, the conformers (**YZ1**–**YZ4**) that have NH_3^+–π interactions are more stable than the conformers (**YZ5**, **YZ6**, **YZ9** and **YZ10**) is where the interactions are lacking. Similar to other monomers, all tyrosine zwitterionic conformations also paired up to four pairs because of the two different orientations of aromatic OH groups. The delicate balance of intra molecular interactions is responsible for the stability of tyrosine zwitterions. In order to see the effect of solvation on **YC** and **YA**, PCM calculations were performed on the three most stable conformers. Solvation brings drastic variation on geometries and relative energies compare to gas-phase geometries. The AIM analysis was carried out to characterize the non-covalent interactions, and this analysis showed BCPs and RCPs at all intramolecular interactions, which were presented in this study. Figure 5 depicts the BCPs of cationic conformations. The ρ values are in the range of 0.0074–0.0442 a.u.

3.5 Tyrosine dimer (**YD**)

The initial conformational space consisted of 74 conformers that were optimized at M05-2X/6-31G(d) level. The initial search resulted in the identification of 67 distinct stationary points. Frequency calculations characterized 59 conformers as minima, seven as transition states and one as higher order saddle points on the potential energy surface. Further single point calculations on these 59 conformers were performed at M05-2X/cc-pVTZ//M05-2X/6-31G(d) level of theory. Table 1 shows the relative energies along with the interaction and reorganization energies at M05-2X level of theory with 6-31G(d) and cc-pVTZ basis sets along with various non-covalent interactions presented in each conformer. Most of the conformers were clustered in the range of 20.00 kcal/mol in both the levels of theory considered in this study. The **YD1** and **YD59** were identified as the most and least stable conformers at both the levels of theory considered in this study. The relative energies are virtually similar and followed same trend in both the levels. The interaction energy can be calculated with respect to the energy of the most stable monomer (IE1) or with respect to the energy of the monomers as present in the dimer conformation (IE2). As expected, IE2 calculated for any conformer is higher than the corresponding IE1. In Table 1, column D shows the IE1, and column E shows the IE2 at M05-2X/6-31G(d) level of theory. If IE1 is considered, then the conformations **YD53**–**YD59** exhibit repulsive interaction energies, whereas no such repulsive interaction was observed in IE2. The difference between the two interaction energies will reflect the change that takes place in the monomer conformation with respect to the most stable conformer during the formation of dimer. Thus, reorganization energy (column E) can vary from 1–18 kcal/mol, higher the reorganization energy, higher is IE2. This analysis indicates that in **YD53**–**YD59**, the monomers are destabilizing by reorganizing its conformation with respect to most stable conformer to stabilize the dimer. In this process, the monomers were destabilized with respect to the global minima. Due to the reorganization of monomers, the conformers **YD53**–**YD59** are showed positive IE1 values. In Table 1, column G and H show the IE1 and IE2 of **YD** at M05-2X/cc-pVTZ//M05-2X/6-31G(d) level of theory, and interaction energy IE1 and IE2 are lower at M05-2X/cc-pVTZ compare to M05-2X/6-31G(d) level of theory. If we consider the IE1 at M05-2X/cc-pVTZ level, three conformers **YD57**–**YD59** are showing repulsive interaction energy; however, there is no such repulsive energies were observed in the case of IE2. BSSE corrected interaction energies have been reported in column I of Table 1 at M05-2X/cc-pVTZ//M05-2X/6-31G(d) level of theory. BSSE corrected interaction energies are slightly lower than M05-2X/cc-pVTZ interaction energies.

Figure 6 shows the principal geometrical parameters and relative energies of the representative 20 conformers (all are given in supporting information) of **YD** at M05-2X/6-31G(d) level of theory. Fig. 6 shows the principal geometrical parameters, electron density rho and relative energy of representative 24 tyrosine dimers at M05-2X/6-31G(d) level of theory. A cursory look at this figure indicates that all dimeric conformers are stabilized by side chain intermolecular interactions. Figure 7 depicts the graph of (A) interaction energy (IE2) and reorganization energy, and graph (B) explains the interaction energy (IE1) with various non-covalent interactions characterized by AIM analysis presented in different tyrosine dimer conformations. The length of each bar corresponds to the interaction energy value of that particular dimer. The different colors in the bar further assist us to identify the nature of various non-covalent interactions for each of the dimer studied. This figure clearly explains that moving from most stable conformer **YD1** to least stable **YD59**, the hydrogen bonding interactions are decreased and other interactions involving aromatic side chain were increased. We can observe the positive interaction energy of **YD53**–**YD59** conformers in the graph (B); these conformers have no hydrogen bonds, and as expected, IE2 of these conformers are positive. Figure 8 depicts the variation of relative energies of **YD** at different levels of theory. At M05-2X level of theory, cc-pVTZ basis set showed lower relative energy than 6-31G(d) basis set relative energies.

Table 1 The relative energy (ΔE in kcal/mol), interaction energy (IE in kcal/mol) and reorganization energy (RE in kcal/mol) of various conformations of tyrosine dimer at various levels of theory

Str.	A	B	C	D	E	F	G	H	I	Non-covalent interactions characterized by AIM analysis
YD1	0.00	0.00	0.00	−17.89	−25.05	7.16	−16.63	−20.61	−14.49	OH/O, OH/OH, OH/OH, CH/O,CH/O, π/π, CH/π
YD2	0.58	2.00	1.94	−17.31	−28.68	11.37	−14.62	−23.58	−12.18	OH/O, OH/N, OH/OH, CH/O, CH/O
YD3	1.78	2.63	2.70	−16.12	−30.05	13.93	−14.00	−24.60	−11.41	OH/O, OH/N, OH/OH, CH/O, NH/π
YD4	2.04	1.89	0.81	−15.86	−24.83	8.98	−14.74	−20.72	−12.38	OH/N, OH/OH, NH/O, CH/OH, OH/π, OH/π
YD5	2.64	2.30	1.87	−15.26	−27.65	12.39	−14.32	−23.12	−11.78	OH/OH, OH/N, CH/O, CH/O, CH/O, OH/π
YD6	3.26	2.91	2.27	−14.63	−27.34	12.70	−13.72	−23.46	−11.31	OH/N, CH/O, CH/O, CH/OH, OH/π, CH/π, π/π
YD7	3.88	3.35	2.36	−14.02	−23.02	9.00	−13.27	−19.08	−11.28	OH/N, NH/O, CH/O, π/π, OH/π
YD8	3.91	3.54	2.42	−13.99	−23.48	9.49	−13.08	−19.37	−10.94	OH/N, OH/OH, CH/O, CH/O, CH/OH, CH/π, CH/π
YD9	3.96	4.04	2.97	−13.94	−26.09	12.14	−12.59	−21.69	−10.19	OH/N, OH/OH, CH/O, CH/OH, CH/π, π/π
YD10	4.63	4.04	3.56	−13.27	−18.95	5.67	−12.59	−16.00	−10.80	OH/O, OH/OH, NH/O, CH/OH, CH/OH, π/π
YD11	4.72	4.47	4.47	−13.18	−24.58	11.40	−12.15	−20.28	−9.92	OH/N, NH/O, CH/O, CH/O, CH/OH, OH/π
YD12	5.55	5.10	3.95	−12.35	−22.72	10.37	−11.53	−18.72	−9.82	OH/N, NH/O, CH/π, OH/π, π/π
YD13	5.78	4.62	4.22	−12.13	−25.44	13.31	−12.00	−21.71	−9.80	OH/O, OH/O, CH/O, CH/O, CH/OH, OH/π, π/π
YD14	5.96	5.83	5.79	−11.95	−24.36	12.41	−10.79	−19.88	−8.68	NH/O, OH/N, CH/O, OH/π
YD15	6.41	5.28	4.77	−11.50	−22.76	11.26	−11.35	−19.29	−9.30	OH/N, CH/O, OH/π, OH/π, CH/π, π/π
YD16	6.46	6.17	5.27	−11.45	−26.71	15.26	−10.46	−22.36	−8.08	OH/N, OH/OH, CH/O, CH/OH, CH/OH, CH/OH, π/π
YD17	6.91	6.68	6.23	−11.00	−24.51	13.52	−9.94	−20.24	−7.76	OH/O, OH/OH, OH/OH, CH/O, CH/OH, NH/π, π/π, π/π
YD18	6.95	5.87	6.71	−10.96	−20.43	9.47	−10.76	−17.00	−9.17	OH/N, CH/O, NH/π
YD19	6.97	6.51	6.47	−10.94	−18.12	7.18	−10.12	−15.16	−8.32	OH/O, OH/OH, CH/O, CH/OH, CH/π, NH/π, NH/π
YD20	7.18	6.95	7.39	−10.73	−18.18	7.45	−9.67	−14.88	−7.75	OH/O, OH/OH, CH/N, π/π
YD21	7.50	6.58	6.56	−10.42	−20.12	9.70	−10.05	−16.78	−8.37	OH/N, CH/O, CH/OH, CH/N
YD22	7.80	6.53	6.66	−10.12	−12.45	2.34	−10.10	−10.51	−8.42	OH/OH, CH/O, CH/O, CH/OH, CH/OH, π/π, NH/π
YD23	7.87	7.56	6.29	−10.04	−26.12	16.07	−9.07	−21.39	−6.02	OH/O, OH/N, NH/O, NH/OH, NH/π, OH/π, CH/π
YD24	8.68	7.63	7.57	−9.24	−21.23	11.99	−9.00	−17.84	−7.41	OH/N, NH/O, CH/OH, π/π, CH/π
YD25	8.73	7.33	7.11	−9.19	−12.35	3.16	−9.30	−10.55	−7.58	NH/N, CH/N, CH/O, OH/π, π/π, CH/π
YD26	9.32	7.92	8.42	−8.60	−18.37	9.77	−8.71	−15.39	−7.11	OH/O, OH/O, OH/π, OH/π
YD27	9.56	9.15	9.11	−8.36	−25.29	16.93	−7.48	−20.75	−5.54	OH/O, OH/N, CH/O, NH/π
YD28	9.69	8.41	8.63	−8.23	−16.29	8.06	−8.22	−12.74	−6.01	OH/OH, NH/N, CH/O, CH/O, CH/N, CH/N, CH/π
YD29	9.91	8.55	9.93	−8.01	−9.41	1.40	−8.08	−7.61	−5.36	OH/OH, CH/OH, CH/OH
YD30	10.17	10.51	11.40	−7.75	−23.58	15.83	−6.12	−18.77	−3.93	OH/O, OH/O, OH/N, CH/O, OH/π
YD31	10.27	8.61	9.51	−7.65	−18.48	10.83	−8.02	−15.56	−6.20	OH/O, CH/O, NH/OH, OH/π, OH/π, π/π
YD32	11.12	9.25	9.33	−6.81	−16.62	9.82	−7.38	−13.98	−5.29	OH/O, NH/O, CH/OH, OH/π, π/π, π/π
YD33	11.35	10.52	10.56	−6.58	−23.66	17.08	−6.11	−19.99	−3.89	OH/OH, NH/O, CH/O, OH/π, CH/π, π/π
YD34	11.37	10.08	8.91	−6.56	−19.68	13.13	−6.55	−16.52	−4.28	NH/O, NH/N, CH/O, CH/O, OH/π, OH/π, CH/π
YD35	11.88	11.25	11.29	−6.05	−24.19	18.14	−5.37	−20.16	−5.55	OH/O, OH/O, OH/OH, CH/O, CH/π, π/π
YD36	11.91	10.08	10.28	−6.02	−19.01	12.99	−6.55	−16.27	−4.81	OH/O, NH/OH, OH/π, CH/π, π/π
YD37	12.59	10.72	11.69	−5.34	−15.19	9.86	−5.90	−12.62	−4.16	NH/O, OH/π, OH/π, CH/π
YD38	13.10	10.82	11.46	−4.83	−12.20	7.36	−5.81	−10.02	−4.21	OH/OH, CH/O, OH/π, π/π
YD39	13.92	11.30	11.78	−4.01	−11.47	7.45	−5.33	−9.33	−3.39	NH/OH, CH/O, CH/N, CH/N, OH/π, NH/π
YD40	13.96	12.20	12.35	−3.97	−16.45	12.48	−4.43	−13.83	−3.07	OH/N, CH/π, π/π
YD41	14.05	12.06	13.27	−3.88	−6.73	2.84	−4.57	−5.62	−3.89	CH/O, CH/O, OH/π, π/π
YD42	14.59	12.75	13.34	−3.34	−14.25	10.90	−3.87	−11.66	−2.52	OH/OH, OH/π OH/π, OH/π, π/π
YD43	15.15	13.13	14.38	−2.78	−12.30	9.52	−3.50	−9.75	−2.14	OH/OH, OH/π, π/π
YD44	15.92	14.55	13.48	−2.02	−16.09	14.07	−2.08	−12.92	−2.12	OH/OH, NH/O, CH/OH, CH/OH, CH/OH, OH/π, π/π
YD45	15.94	13.26	14.45	−2.00	−11.49	9.49	−3.37	−9.62	−2.11	CH/O, OH/π, OH/π, π/π

Table 1 continued

Str.	A	B	C	D	E	F	G	H	I	Non-covalent interactions characterized by AIM analysis
YD46	16.09	13.38	13.96	−1.85	−11.66	9.80	−3.24	−9.59	−1.70	NH/O, NH/N, CH/O, CH/O, π/π
YD47	16.11	12.95	14.29	−1.84	−8.27	6.44	−3.67	−6.61	−2.56	OH/OH, π/π
YD48	16.17	14.26	13.71	−1.77	−17.41	15.64	−2.37	−14.02	−0.33	OH/OH, CH/O, CH/O, CH/O, NH/O, OH/π, π/π, CH/π
YD49	17.03	15.08	14.92	−0.91	−13.20	12.29	−1.55	−10.68	0.04	NH/N, CH/O, CH/O, CH/O, OH/π
YD50	17.04	15.27	15.91	−0.90	−15.60	14.70	−1.36	−12.77	0.62	OH/O, OH/O, CH/O, CH/O, CH/O, CH/N, OH/π, NH/π
YD51	17.09	13.92	15.91	−0.85	−8.79	7.94	−2.71	−7.23	−1.24	NH/N, NH/CH, OH/π, π/π, CH/π, CH/π
YD52	17.44	15.07	14.24	−0.50	−15.61	15.10	−1.56	−12.71	−0.02	OH/OH, CH/O, OH/π, OH/π, OH/π, π/π, CH/π
YD53	18.21	15.80	17.10	0.27	−12.50	12.77	−0.82	−10.45	0.78	OH/OH, CH/O, OH/π, OH/π, OH/π, CH/π
YD54	19.13	16.00	14.44	1.18	−15.45	16.63	−0.62	−12.77	1.46	OH/OH, NH/O, CH/O, CH/O, OH/π, OH/π, π/π, CH/π
YD55	19.40	16.38	16.50	1.45	−14.58	16.03	−0.24	−12.36	1.60	CH/O, CH/O, CH/O, CH/OH, CH/N, OH/π
YD56	19.45	16.03	17.36	1.50	−7.46	8.96	−0.59	−6.35	2.10	OH/π, π/π
YD57	22.56	19.19	17.96	4.60	−9.56	14.16	2.56	−8.45	2.55	CH/OH, CH/OH, NH/π, NH/π, CH/π, CH/π, CH/π
YD58	22.90	19.22	21.11	4.94	−7.00	11.94	2.59	−6.12	3.39	CH/OH, OH/π
YD59	23.86	20.07	22.04	5.90	−6.14	12.04	3.45	−5.39	3.50	OH/π, CH/π

A: relative energy at M05-2X/6-31G(d); B: relative energy at M05-2X/cc-pVTZ//M05-2X/6-31G(d); C: relative energy at B3LYP-D/cc-pVTZ//M05-2X/6-31G(d); D: interaction energy (IE1) at M05-2X/6-31G(d); E: interaction energy (IE2) at M05-2X/6-31G(d); F: reorganization energy (RE); G: interaction energy (IE1) at M05-2X/cc-pVTZ//M05-2X/6-31G(d); H: interaction energy (IE2) at M05-2X/cc-pVTZ//M05-2X/6-31G(d); I: interaction energy (IE1) at M05-2X/cc-pVTZ//M05-2X/6-31G(d) (BSSE corrected)

Figure 8 also shows relative energy values for geometries at B3LYP-D/cc-pVTZ//M05-2X/6-31G(d) level to include dispersion correction. It is obvious from the figure that only a minor variation in relative energy ($\leq$2.00 kcal/mol) is noticed between dispersion corrected B3LYP/cc-pVTZ and M05-2X/cc-pVTZ levels of theory in the majority of conformations studied. The MP2/6-31G(d)//M05-2X/6-31G(d) relative energy showed slightly higher relative energy compare to other levels of theory. It is obvious from the figure that dispersion corrected relative energies are almost similar to M05-2X/cc-pVTZ level of theory, as expected MP2 method is over estimating the energies in the case of dimer compare to other methods considered in this study. As we expected, cc-pVTZ basis set showed higher interaction energy than interaction energy of 6-31G(d) basis set (Table 1). The presence of two hydrogen bond donors (COOH, NH_2) and three hydrogen bond acceptors (C=O, C(O)OH and NH_2) in tyrosine conformers allows for a wide range of hydrogen bonding combinations. Consistent with the typical intramolecular interaction distances found in this system, a distance of 2.80 Å was used as a cut off for the near-atom interaction between the NH_2 group and the carboxyl. Analyzing the stable conformers obtained, we find nine types of hydrogen bonds between the amino group and the carboxyl groups, namely OH–OC, OH–N, OH–OH, NH–O, NH–N, NH–OH, CH–O, CH–N and CH–OH. The AIM analysis has been performed to characterize the non-covalent interactions presented in the **YD**. AIM analysis showed BCPs and RCPs at non-covalent interactions presented in tyrosine dimers. The AIM analysis reveals that OH–N type of hydrogen bonds have higher electron density rho (ρ in a.u.) and electron density laplacian ($\nabla^2\rho$ in a.u.) values $\sim$0.0659 and 0.0329, respectively, than other interactions presented in this study. The OH–N, OH–O and OH–OH interactions showed higher ρ and $\nabla^2\rho$ values 0.066–0.033, 0.034–0.028 and 0.039–0.031, respectively, than other hydrogen bonding interactions presented in this study. The OH–N, NH–N and CH–N interactions have more ρ and $\nabla^2\rho$ values than OH–O/OH, NH–O/OH and CH–O/OH interactions. This indicates that nitrogen is a better proton acceptor than oxygen. In this study, the interactions between side chain and aromatic moiety such as OH–π, NH–π and CH–π interactions and π–π interactions are presented in almost all tyrosine dimer conformations. As we expected, these interactions showed less ρ and $\nabla^2\rho$ values than different hydrogen bonds. The parallel displaced (PD) and T-shaped interactions were presented in most of the conformations, as expected there is no face-to-face stacking conformation in this study. For most of the hydrogen bonds presented in this study, ρ and $\nabla^2\rho$ values are in the range of conventional hydrogen bonds. The topological analysis of the electron density has been a fairly reliable model to try to understand the chemical

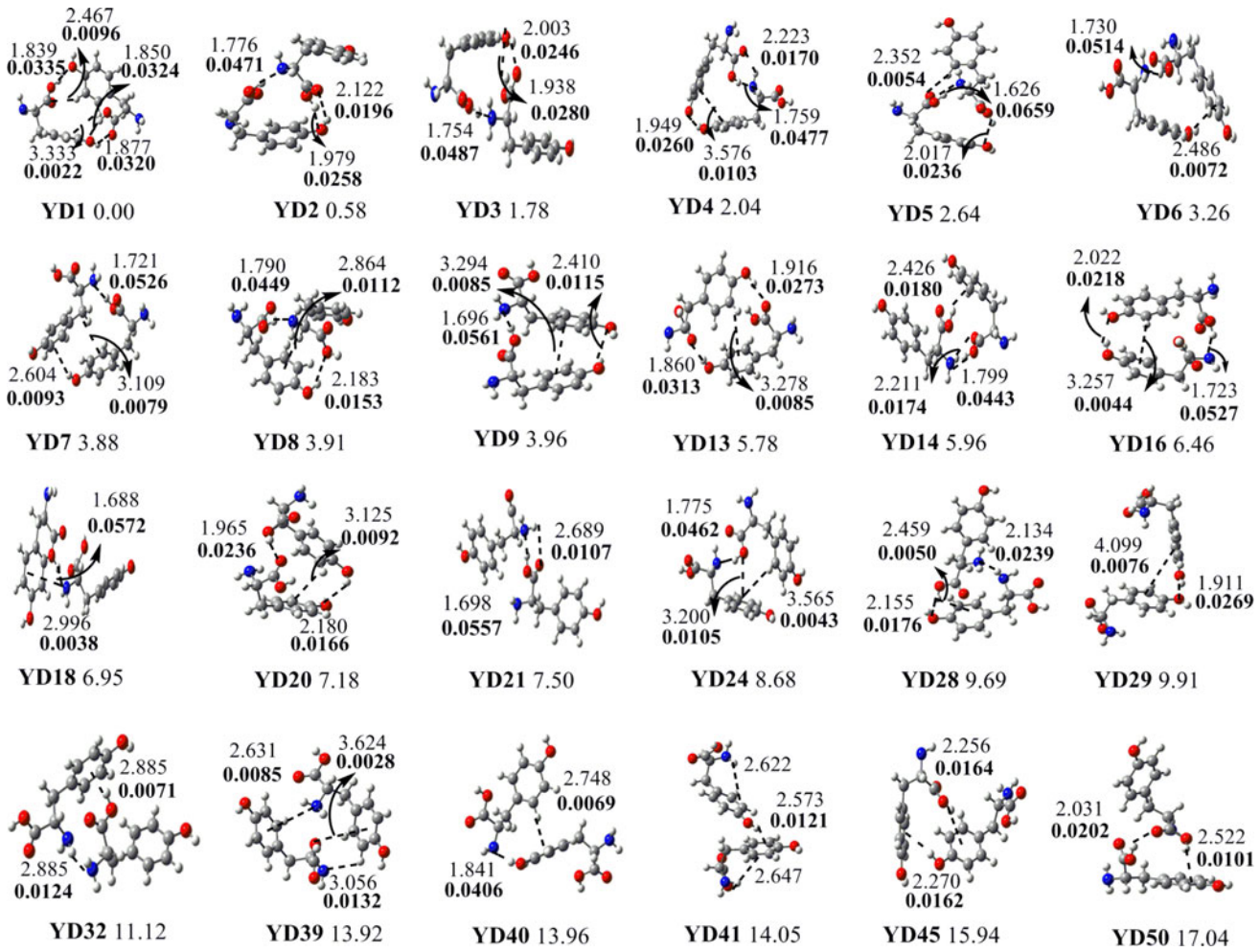

Fig. 6 The principal geometrical parameters (in Å), electron density rho (ρ in a.u. bold) and relative energy (in kcal/mol) of representative 24 tyrosine dimers at M05-2X/6-31G(d) level of theory (all 59 conformers are given in the supporting information)

interactions concept. However, like any model, this model also has its own limitations [67–70], but we feel that such limitations are not applicable to the type of study in this manuscript. The majority of the conformers are stabilized by hydrogen bonding interactions in addition to other interactions like OH–π, NH–π, CH–π and π–π that arise from the side chain interaction. Moving from **YD1**–**YD59**, the hydrogen bonding interactions are decreased and other interactions are increased.

4 Conclusions

The study reports the most comprehensive study on the tyrosine dimers and the conformational analysis of tyrosine monomers, cations, anions and zwitterions. The conformational search of monomers characterized as 38, 12, 14 and 9 distinct conformations on potential energy surface of neutral, anion, cation and zwitterions, respectively. Due to the presence of OH group on aromatic ring, all forms of tyrosine conformations have appeared in pairs. The AIM analysis characterized the nature of various non-covalent interactions such as hydrogen bonds, NH–π, OH–π and CH–O interactions that stabilized all monomers. A close examination of the energetics of the various conformers with different basis set, it was clear that the trends obtained with various basis sets are very similar. However, the relative energies and the span of the variations are slightly smaller with cc-pVTZ basis set. Fifty-nine dimers are characterized as minima on the potential energy surface. The **YD** was stabilized by nine different hydrogen bonds between carboxylic and amino groups and OH–π, NH–π, CH–π and π–π interactions. The monomers undergo drastic variation from the most stable conformation during the formation of the dimer, which is reflected by their higher reorganization energy.

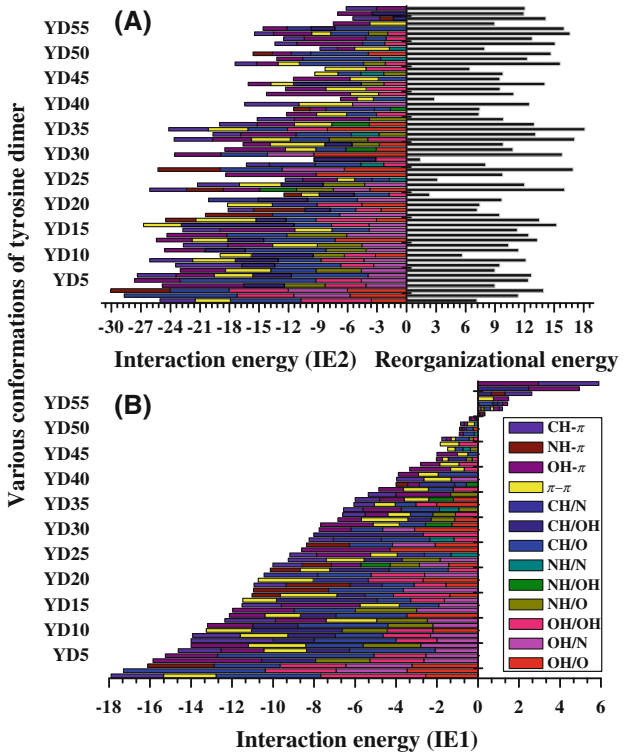

Fig. 7 The graph of **a** interaction energy (IE2 in kcal/mol), reorganization energy, **b** interaction energy (IE1 in kcal/mol) and different non-covalent interactions characterized by AIM analysis presented in various conformations of tyrosine dimers at M05-2X/6-31G(d) level of theory. The various conformations of tyrosine dimers, **YD1** to **YD59**, are given. Every fifth dimer is mentioned on Y-axis for clarity

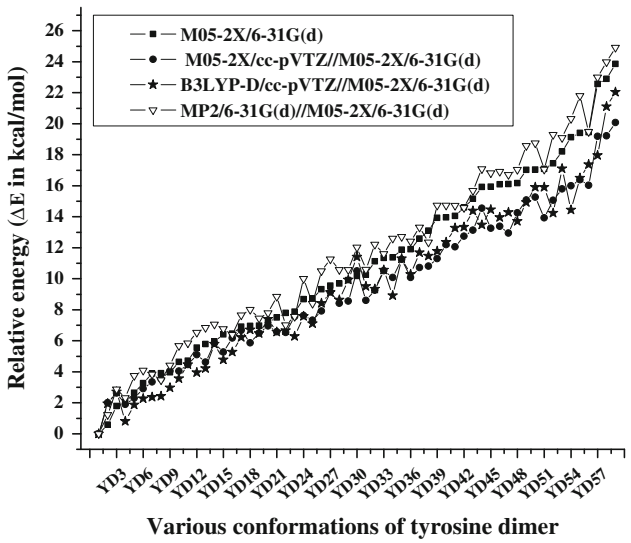

Fig. 8 The relative energy (ΔE in kcal/mol) of various conformations of tyrosine dimer with respect to **YD1** at various levels of theory

Acknowledgments We thank CSIR for financial support and also NWP0053 project. UP thanks CSIR, New Delhi for junior research fellowship. DST is thanked for Swarnajayanthi Fellowship to GNS.

References

1. Furst P, Stehle P (2004) J Nutr 134:1558–1565
2. Lieberman HR, Corkin S, Spring BJ, Wurtman RJ, Growdon JH (1985) Am J Clin Nutr 42:366–370
3. Martinez SJ III, Alfano JC, Levy DH (1992) J Mol Spectrosc 156:421–430
4. Lindinger A, Toennies JP, Vilesov AF (1999) J Chem Phys 110:1429–1436
5. Li L, Lubman DM (1988) Appl Spectrosc 42:418–424
6. Grace LI, Cohen R, Dunn TM, Lubman DM, de Vries MS (2002) J Mol Spectrosc 215:204–219
7. Cohen R, Brauer B, Nir E, Grace L, de Vries MS (2000) J Phys Chem A 104:6351–6355
8. Meiling Z, Huang Z, Lin Z (2005) J Chem Phys 122:134313–134319
9. Reddy AS, Sastry GN (2005) J Phys Chem A 109:8893–8903
10. Reddy AS, Sastry GM, Sastry GN (2007) Proteins: Struct Funct Bioinform 67:1179–1184
11. Mahadevi AS, Sastry GN (2011) J Phys Chem B 115:703–710
12. Neela YI, Mahadevi AS, Sastry GN (2010) J Phys Chem B 114:17162–17171
13. Stearns JA, Mercier S, Seaiby C, Guidi M, Boyarkin OV, Rizzo TR (2007) J Am Chem Soc 129:11814–11820
14. Boyarkin OV, Mercier S, Kamariotis A, Rizzo TR (2006) J Am Chem Soc 128:2816–2817
15. Kang H, Jouvet C, Dedonder-Lardeux C, Martrenchard S, Gregoire G, Desfrancois C, Schermann JP, Barat M, Fayeton JA (2005) Phys Chem Chem Phys 7:394–398
16. Gregoire G, Jouvet C, Dedonder C, Sobolewski AL (2007) J Am Chem Soc 129:6223–6231
17. Dinadayalane TC, Sastry GN, Leszczynski J (2006) Int J Quantum Chem 106:2920–2933
18. Gao B, Wyttenbach T, Bowers MT (2009) J Am Chem Soc 131:4695–4701
19. O'Hair RAJ, Bowie JH, Gronert S (1992) Int J Mass Spectrom Ion Proc 117:23–36
20. Woo HK, Lau KC, Wang XB, Wang LS (2006) J Phys Chem A 110:12603–12606
21. Tian Z, Kass SR (2008) J Am Chem Soc 130:10842–10843
22. Tian Z, Pawlow A, Poutsma JC, Kass SR (2007) J Am Chem Soc 129:5403–5407
23. Jones CM, Bernier M, Carson E, Colyer KE, Metz R, Pawlow A, Wischow ED, Webb I, Andriole EJ, Poutsma JC (2007) Int J Mass Spectrom 267:54–62
24. Oomens J, Steill JD, Redlich B (2009) J Am Chem Soc 131:4310–4319
25. Nielsen PA, Norrby PO, Liljefors T, Rega N, Barone V (2000) J Am Chem Soc 122:3151–3155
26. Jockusch RA, Lemoff AS, Williams ER (2001) J Am Chem Soc 123:12255–12265
27. Tajkhorshid E, Jalkanen KJ, Suhai S (1998) J Phys Chem B 102:5899–5913
28. Rijs AM, Ohanessian G, Oomens J, Meijer G, von Helden G, Compagnon I (2010) Angew Chem Int Ed 49:2332–2335
29. Scheiner S, Kar T, Pattanayak J (2002) J Am Chem Soc 124:13257–13264
30. Chipot C, Jaffe R, Maigret B, Pearlman AD, Kollman PA (1996) J Am Chem Soc 118:11217–11224
31. Hobza P, Selzle HL, Schlag EW (1994) J Am Chem Soc 116:3500–3506
32. Chourasia M, Sastry GM, Sastry GN (2011) Int J Biol Macromol 48:540–552
33. Mahadevi AS, Anuja PR, Gadre SR, Sastry GN (2010) J Chem Phys 133:164308–164319

34. Hobza P, Riehn C, Weichert A, Brutschy B (2002) J Chem Phys 283:331–339
35. Sagarik K, Asawakun P (1997) J Chem Phys 219:173–191
36. Bohm HJ, Ahlrichs R (1982) J Chem Phys 77:2028–2035
37. Connell LL, Ohline SM, Joireman PW, Corcoran TC, Fleker PM (1992) J Chem Phys 96:2585–2593
38. Sinnokrot MO, Sherrill CD (2003) J Phys Chem A 107:8377–8379
39. Mooney DA, Muller-Plathe F, Kremer K (1998) Chem Phys Lett 294:135–142
40. Chelli R, Gervasio FL, Procacci P, Schettino V (2002) J Am Chem Soc 124:6133–6143
41. Munshi P, Guru Row TN (2005) J Phys Chem A 109:659–672
42. Mahadevi AS, Neela YI, Sastry GN (2011) Phys Chem Chem Phys, doi:10.1039/C1CP21346F (in press)
43. Umadevi D, Sastry GN (2011) J Phys Chem Lett 2:1572–1576
44. Umadevi D, Sastry GN (2011) J Phys Chem C 115:9656–9667
45. Vijay D, Sastry GN (2006) J Phys Chem A 110:10148–10154
46. Rao JS, Zipse H, Sastry GN (2009) J Phys Chem B 113:7225–7236
47. Nagaraju M, Sastry GN (2009) J Phys Chem A 113:9533–9542
48. Ma JC, Dougherty DA (1997) Chem Rev 97:1303–1324
49. Meyer EA, Castellano RK, Diederich F (2003) Angew Chem Int Ed 42:1210–1250
50. Burley SK, Petsko GA (1986) FEBS Lett 203:139–143
51. Vijay D, Sastry GN (2010) Chem Phys Lett 485:235–242
52. Vijay D, Zipse H, Sastry GN (2008) J Phys Chem B 112:8863–8867
53. Reddy AS, Vijay D, Sastry GM, Sastry GN (2006) J Phys Chem B 110:2479–2481
54. Reddy AS, Zipse H, Sastry GN (2007) J Phys Chem B 111:11546–11553
55. Rao JS, Dinadayalane TC, Leszczynski J, Sastry GN (2008) J Phys Chem A 112:12944–12953
56. Purushotham U, Vijay D, Sastry GN (unpublished results)
57. Tomasi J, Mennucci B, Camm R (2005) Chem Rev 105:2999–3093
58. Grimme S (2006) J Comput Chem 27:1787–1799
59. Grimme S (2006) J Chem Phys 124:034108
60. Boys SF, Bernardi R (1979) Mol Phys 19:553–566
61. Bader RFW (1990) Atoms in molecules a quantum theory. Oxford University Press, Oxford
62. Gaussian 03, Revision D.1Frisch MJ, Trucks GW, Schlegel HB, Scuseria GE, Robb MA, Cheeseman JR, Montgomery JA, Vreven Jr.T, Kudin KN, Burant JC, Millam JM, Iyengar SS, Tomasi J, Barone V, Mennucci B, Cossi M, Scalmani G, Rega C, Petersson GA, Nakatsuji H, Hada M, Ehara M, Toyota K, Fukuda R, Hasegawa J, Ishida M, Nakajima T, Honda Y, Kitao O, Nakai H, Klene M, Knox X, Li JE, Hratchian HP, Cross JB, Adamo C, Jaramillo J, Gomperts R, Stratmann RE, Yazyev O, Austin AJ, Cammi R, Pomelli C, Ochterski JW, Ayala PY, Morokuma K, Voth GA, Salvador P, Dannenberg JJ, Zakrzewski VG, Dapprich S, Daniels AD, Strain MC, Farkas O, Malick DK, Rabuck AD, Raghavachari K, Foresman JB, Ortiz JV, Cui Q, Baboul AG, Clifford S, Cioslowski J, Stefanov BB, Liu G, Liashenko A, Iskorz P, Komaromi I, Martin RL, Fox DJ, Keith T, Al-Laham MA, Peng CY, Nanayakkara A, Challacombe M, Gill PMW, Johnson B, Chen W, Wong MW, Gonzalez C, Pople JA (2003) Gaussian, Inc. Pittsburgh PA
63. Ebrahimi A, Mostafa HK, Gholipour AR, Masoodi HR (2009) Theor Chem Acc 124:115–122
64. Julian RR, Beauchamp JL, Goddard WA III (2002) J Phys Chem A 106:32–34
65. Forbes MW, Bush MF, Polfer NC, Oomens J, Dunbar RC, Williams ER, Jockusch RA (2007) J Phys Chem A 111:11759–11770
66. Fei W, Rai AK, Lu Z, Lin Z (2009) Theochem 895:65–71
67. Cerpa E, Krapp A, Moreno RF, Donald KJ, Merino G (2009) Chem Eur J 15:1985–1990
68. Cerpa E, Krapp A, Vela A, Merino G (2008) Chem Eur J 14:10232–10234
69. Krapp A, Frenking G (2007) Chem Eur J 13:8256–8270
70. Bader RFW (2009) J Phys Chem A 113:10391–10396